MATHEMATICAL BIOSCIENCES
AND ENGINEERING
Volume **10**, Number **3**, June **2013**

doi:10.3934/mbe.2013.10.729

pp. **729–742**

HYBRID DISCRETE-CONTINUOUS MODEL OF INVASIVE BLADDER CANCER

Eugene Kashdan

School of Mathematical Sciences, Tel Aviv University
Tel Aviv, Ramat Aviv, 69978, Israel

Svetlana Bunimovich-Mendrazitsky

Department of Computer Science and Mathematics
Ariel University Center of Samaria
Ariel, 40700, Israel

Abstract. Bladder cancer is the seventh most common cancer worldwide. Epidemiological studies and experiments implicated chemical penetration into urothelium (epithelial tissue surrounding bladder) in the etiology of bladder cancer. In this work we model invasive bladder cancer. This type of cancer starts in the urothelium and progresses towards surrounding muscles and tissues, causing metastatic disease. Our mathematical model of invasive BC consists of two coupled sub-models: (i) living cycle of the urothelial cells (normal and mutated) simulated using discrete technique of Cellular Automata and (ii) mechanism of tumor invasion described by the system of reaction-diffusion equations. Numerical simulations presented here are in good qualitative agreement with the experimental results and reproduce in vitro observations described in medical literature.

1. **Introduction.** Bladder cancer (BC) is a worldwide problem. It is estimated that 386 300 new cases and 150 200 deaths from BC occur each year, with the highest incidence in industrialized and developed countries [16]. Tobacco smoking is the most important BC risk factor. Another significant risk factors are occupational exposure to carcinogens such as aromatic amines in chemicals and contaminants in drinking water [22].

The BC is known to be a multistage disease as the number of events are required for tumor development. The process also known as *carcinogenesis* starts when the chemicals known as *carcinogens* penetrating from the bladder lumen affect top (umbrella) cells of the urothelium as shown in Fig. 1.

Subsequently they reach the deeper layers of the tissue (intermediate and basal cells). That may last several years until the carcinogenic substance accumulates in the urothelium above the threshold level sufficient to trigger the sequence of the DNA mutations leading to the tumor growth [17, 38]. The stages (and types) of BC are shown in Fig. 2.

The most complicated and dangerous form of BC – invasive BC affects about 25% of patients. Treatment of invasive BC often requires removal of the bladder (cystectomy) to prevent the tumor from spreading to the lungs, liver, and bone

2010 *Mathematics Subject Classification.* Primary: 92C42; Secondary: 35K57, 37B15.

Key words and phrases. Bladder cancer, metaloproteinases, cellular automata, reaction-diffusion equations.

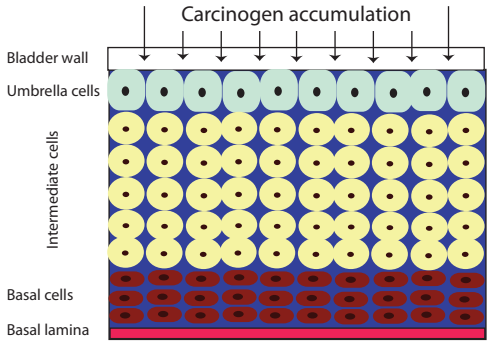

FIGURE 1. The structure of the urhotelium

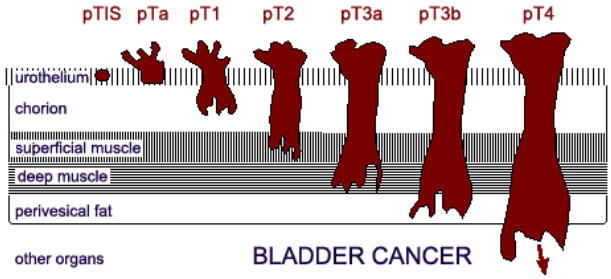

FIGURE 2. BC stages according to [3]

[26]. The goal of our studies is to understand quantitatively the mechanism of tumor invasion and examine pathways leading to this form of BC.

Invasion occurs at the tumor-host interface, where the tumor and the stromal cells exchange enzymes and cytokines that modulate the local extracellular matrix (ECM) and stimulate cell migration. The most important group of ECM degrading enzymes is known as the matrix metalloproteinases (MMP) [5, 7, 20]. The action of MMP leads to the breakdown of connective tissue barriers [32].

The nearby healthy tissue responds to MMP secretion by producing tissue inhibitors of metalloproteinases (TIMP), which neutralize the degrading enzymes [33]. The progress of invasive BC depends on the MMP-TIMP interaction. Shifting the balance towards MMP secretion leads to advance of malignant cells towards the nearby tissue and subsequent metastasis. Presence of the MMP has been experimentally observed on the various stages of the high-grade (stages T2–T4 in the Fig. 2) BC [27, 36].

Mathematical modeling of cancer invasion is discussed in the number of publications ([1, 8, 11, 21, 28, 30, 35] and review in [29]). The models of enzyme-inhibitor interaction as a driving force behind the tumor invasion were, in particular, proposed in [8, 28, 30, 35]. Our work is the first one that takes into account the specifics of BC and includes the major factors leading to its invasive form.

There are three basic approaches to modeling cancer invasion:

- The most widely used models are involving Cellular Automata (CA) for simulation of cell living cycle and they are often combined with the sub-models, which could include oxygen and nutrients delivery [11] and/or PDE-based sub-models for interaction of the peripheral cancer cells with the ECM to model tumor invasion on the local level [1]. The theoretical studies of such models are very complicated due to their hybrid nature. However, following the number of assumptions and simplifications in [30], the authors have found the analytical solution to model equations using Fourier analysis.
- The second approach is pure continuous and it is based on the hypothesis of competition for space between the tumor cells and the nearby healthy tissue. The process is modeled using traveling waves approach [21, 28] with addition of diffusion to stabilize the numerical solution. We adopt this approach as a way to explain the number of qualitative factors leading to the BC invasion. The models of this type presented in the literature are usually one-dimensional and their theoretical analysis is done on the basis of the asymptotic expansions in the vicinity of the tumor-tissue interface.
- The third approach to modeling tumor invasion comes from the statistical mechanics and it involves multiple Monte-Carlo runs to compute the average speed and depth of tumor propagation [35]. The basis of these discrete models is Potts model and its extensions [14].

In our approach we use CA to model cell living cycle. CA allows us to model intuitively the tissue regulatory mechanisms: cell proliferation, apoptosis, and dynamics of both regular and mutated cells [10].

We include specific to BC carcinogen penetration sub-model as a major factor leading to the adoption of cancer phenotype by the regular cells (see [18] for its description). We expand to two dimensions the protease-inhibitor interaction model suggested by Byrne et al. for simulation of trophoblast invasion [6]. The combination of CA and MMP-TIMP interaction models is done by using the ECM degradation criteria proposed in [35] following in vitro experimental results discussed in [24].

In this work, we are trying to look on the tumor invasion from the experimental biologist perspective. We make series of observations and measurements using our computational model instead of the microscope. In such a framework, both the tumor cells and the tissue cells are modeled as discrete objects reacting on the continuous processes (carcinogen penetration and MMP-TIMP interaction). The cell status is amended on the daily basis and reflected in the model output. The models communicate using continuous (MMP, TIMP and carcinogen concentration) and discrete (tumor and tissue cell densities) parameters.

The manuscript is organized as follows. In the next section we give a description of the discrete CA model adapted to the modeling of living cycle of the urothelial cells. We also give a brief overview of the carcinogen penetration model suggested in [18]. The section three is dedicated to the continuous model of the MMP-TIMP interaction including its theoretical basis and the references to the experimental results, where it is possible. The section four discusses the combination of the models. The section five includes results of the numerical simulations and analysis of the qualitative data using quantitative approach. The paper is wrapped up by the conclusions and directions for future research.

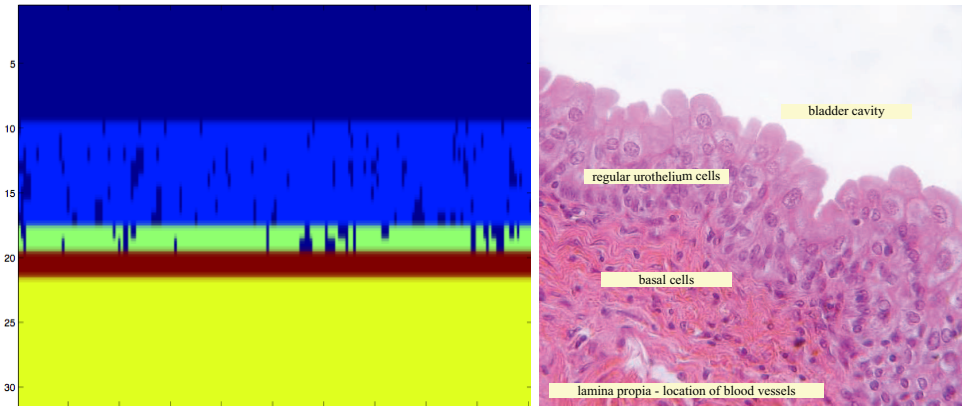

FIGURE 3. Modeled slice of normal urothelium (*left*) and actual image of the urothelium obtained from the cystoscopy [34] (*right*). The colors on the left plot represent: *dark blue* – the bladder cavity and the empty space following the cell death inside the urothelium; *light blue* – regular urothelium cells (intermediate and umbrellas cells); *green* – the basal cells; *red* – bordering urothelium lamina propia, the part of the bladder system, which includes the blood vessels; *yellow* – muscle and fat layers

2. **Computational model of cell dynamics.** CA model is used to simulate carcinogenesis in urothelium and tumor invasion. The basic structure of the model is a two-dimensional grid, which represents a slice of the bladder tissue under consideration as shown in Fig. 3.

The model consists of a 2D array of automaton elements, which will be eventually identified with the real urothelial cells. The state vector, whose components correspond to the features of interest, defines the state of each element. In the model implemented in this work, the *state vector* has six components:

1. cell location: lumen (polyp level), umbrella and transitional level, basal membrane, fat and muscle levels;
2. occupancy type, i.e. whether the element is occupied by the regular cell, the mutated cell, by the "empty space" or by the vessel or tissue;
3. cell status, i.e. whether the cell is in a proliferative or in a quiescent state;
4. the level of carcinogen concentration;
5. mutation counter (zero for normal cells);
6. the ECM degradation level.

The state vector evolves according to the prescribed local rules, used to update any given element from its own state and that of its neighbors on the previous time step.

The structure called "urothelium state" is assigned every cell and it is updated during the numerical simulation. A time-scale is assigned to each iteration of the algorithm and the duration of the cell cycle is considered to be the same for both regular and mutated cells.

In vitro experiments show that invasive cells are less adhesive, more highly mobile, more metabolically active, and more highly mitotic than normal cells [35], so

does our model. In particular, our model represents very important differences in the behavior of regular (normal) and mutated (cancer) cells:

- **Normal cells.** Regular urothelial cells have very slow proliferation rate (their natural turnover time is approximately one year and entrance to the proliferative state occurs approximately six month after the cell birth). The basal (stem) cells of the urothelium proliferate and replace the dead or injured cells in all the layers while accepting the corresponding to each layer phenotype. In average, the normal cell proliferates three times during its living cycle.
- **Cancer cells.** The cancer cell behavior differs from the normal cell rules. Cancer cells are much more resistant to hypoxia and have one more "sleeping" phase in their living cycle. Proliferation rate of cancer cell is higher compared to the regular cell. Cancer cells have usually the apoptosis gene suppressed and, in principle, they can proliferate infinite number of times. The cancer cells are usually more mobile than the regular cells. They could switch the layer occupation during their living cycle, while in the regular cells this possibility is reserved to a very small class of the stem cells, known as "stromal fibroblasts".

The following CA operations (also defined as **CA rules** are applied to each cell as the algorithm progresses from the time-step N to the time-step $N+1$ (one iteration per day):

1. Each new cell enters the quiescent state after its birth. Only on the 6×30^{th}-iteration, the cell passes to the proliferative state. If there are two empty neighboring sites, the cell is ready to proliferate in the next iteration;
2. If the cell is in the proliferative state, it will divide to form two daughter cells, which will move into two neighboring "empty" sites; the daughter cells will be placed on two randomly selected sites of the eight nearest neighboring sites within the same layer inside the urothelium, in accordance with Fig. 3; biologically based assumption [12, 31] is that the cell can proliferate between 6×30^{th}, and 8×30^{th} iteration of its living cycle. Proliferation rate of the cancer cell is higher than the normal cell – in our model the cancer cell can proliferate starting from the $(4 \times 30)^{th}$ iteration of its living cycle.
3. The daughter cells inherit the mutation counter from the mother cells, but not its carcinogen concentration level; mutations that lead to secretion of MMP are marked with a unique MMP-flag in the state vector. If MMP-flag is presented in cancer cells then the promotion of cancer will be develop to direction of blood vessels and hence character of cancer will be invasive. This means that cells with this flag affect the surrounding cell death occurring on their way to the blood vessels.
4. The proliferation stage is followed by the degradative state of the cell that continues 3×30^{th} iterations. On the 12×30^{th} iteration the cell dies, and as a result there is an empty site in the lattice.

3. Model of MMP-TIMP interaction.

3.1. **Background.** Tumor invasion is a complex process involving multiple mechanisms. In the model presented in this section we focus our attention on key parameters involved in early tumor invasion, namely, cancer cells, proteinases (MMP), inhibitors (TIMP) and invaded tissue.

Urothelial cells both normal and mutated live in a complex micro-environment that includes the extracellular matrix (ECM). Out of 13 known types of MMP two (MMP-2 and MMP-9) are characterized by ECM-degrading activity. In particular, MMP-9 is associated with destroying basement membrane and speeding-up tumor metastasis in BC [27, 36].

The main trigger of the invasive BC is a cell mutation, which leads to the MMP secretion by the affected cells. In fact, the process is more complicated (see also [25]) and the assumptions we made here are discussed in the Section 5.1. The cell mutations are random and our approach to the choosing of mutation type is probabilistic.

Following [6] we denote the tumor density as n, the MMP concentration as u, TIMP concentration by v, and invaded tissue density as r. In the simulations presented in Section 5, we consider two-dimensional geometry, however the model could run in three dimensions as well. The equations describe the evolution of n, u, v, and r in space and in time and derived using the mass conservation principle.

3.2. **Cancer cells.** We assume in accordance with [6] that the cancer cells exhibit a small degree of random motion D_n and respond chemotactially to the spatial gradients of the inhibitor with chemotactic coefficient χ. Our approach to the modeling invasive BC is supposed to be physically meaningful. So we employ nonlinear diffusion to describe random motion. Following [18, 37] we choose $D_n \propto n^p$, $(p \geq 1)$. The idea behind the choice of D_n is to keep the speed of the tumor cell propagation finite and the preserve the compact support of the initial data. Applying classical linear diffusion theory to modeling tumor growth is physically incorrect as it predicts infinite speed of propagation [2].

The *in vitro* observations [13] confirm chemotactic response of ECM degraded by the MMP. There is no such observations in BC, however, our suggestion that similar processes happen there and the degraded tissue issues chemicals to which cancer cells respond chemotactically. From modeling point of view it means that we expect to see rising localized gradient in chemoatractant as part of the tumor invasion dynamics.

We assume also in accordance with [6] that tumor proliferation in absence of tissue ($r = 0$) satisfies a logistic growth law with rate parameter k_1 and carrying capacity scaled to unity. The presence of tissue leads to the competition for space between the tumor and tissue it is trying to invade and this could be modeled by crowding term proportional to the product nr. The equation has a following form:

$$\frac{\partial n}{\partial t} = \underbrace{D_n \nabla(n^2 \nabla n)}_{random\ motility} - \underbrace{\chi \nabla(n \nabla v)}_{chemotaxis} + \underbrace{k_1 n(1-n-r)}_{proliferation} \tag{1}$$

3.3. **MMP.** We assume that diffusion coefficient of proteinases D_u is space-dependent and the MMP secretion rate is given by $k_2 n(1-n)$, This term localizes MMP secretion with the front of the invading tumor and it consistent with the experiments [27]. In addition, we assume that the MMP is neutralized by the TIMP as one-to-one reaction, which occurs at rate $k_3 uv$.The MMP equation has a form:

$$\frac{\partial u}{\partial t} = \underbrace{\nabla(D_u \nabla u)}_{diffusion} + \underbrace{k_2 n(1-n)}_{secretion} - \underbrace{k_3 uv}_{neutralization} \tag{2}$$

3.4. **TIMP.** We consider a single general chemo-attractant to neutralize MMP. We assume the inhibitor diffuses with the space-dependent diffusion coefficient D_v, and it is produced by the part of the tissue degraded by the MMP. We also assume that the inhibitor neutralizes proteinases with one-to-one reaction. Defining the rate of the inhibitor production as k_4ur we obtain

$$\frac{\partial v}{\partial t} = \underbrace{\nabla(D_v \nabla v)}_{diffusion} + \underbrace{k_4 ur}_{production} - \underbrace{k_3 uv}_{neutralization} \tag{3}$$

3.5. **Invaded tissue.** Neglecting the random motion of the underlying tissue we assume that it is degraded by the MMP and proliferates while competing for space with the tumor similar to the behavior described in (1). In the other words, in absence of the tumor cells the tissue undergoes logistic growth. However the presence of tumor leads to the competition for spaces between the two types of cells, which we model again by the incorporating the crowding term into logistic growth. Using a modified logistic growth term with rate constant k_5 to describe tissue growth and adding a tissue degradation term $-k_6ur$ we have

$$\frac{\partial r}{\partial t} = \underbrace{k_5 r(1-n-r)}_{tissue\ growth} - \underbrace{k_6 ur}_{degradation} \tag{4}$$

3.6. **Boundary and initial conditions.** We consider a rectangular geometry, where vertical direction passes through the layers of urothelium. We impose no-flux boundary conditions for each dependent variable in all directions.

Our initial condition is dependent on the information obtained from the CA simulation on each time step. The initial condition at time $t = i\Delta t$ includes values of u and v from the previous CA time iteration; r computed as multiplication of latest r by the binary matrix, where zero corresponds to the cells, which ECM degradation led to their apoptosis; n is a binary matrix, which corresponds to the living cells with invasive phenotype at the beginning of the CA time step.

4. **Model interaction.** Initially we consider a normally functioning urothelium, which is surrounded by the bladder lumen (considered as an empty space), basal lamina (location of blood vessels supporting urothelial cells with nutrients and oxygen) and muscle and fat layers as described in Fig. 1. These process is governed by the CA algorithm. A cell state is changing in response to the cell current state and its local neighborhood. Cells attempt to divide at each time step according to the corresponding CA rules for normal cells as discussed in Section 2.

However, the carcinogen penetration through the bladder wall could lead to the sequence of the DNA mutations (as discussed in [18]) and subsequent change of cell phenotype. The carcinogen concentration at each cell is computed as the solution to the nonlinear diffusion equation derived in [18] from the Porous Medium Equation [37] averaged over the cell area.

Continuous in time and in space simulation of carcinogen penetration supplies the CA model with carcinogen concentration level for each cell and reacts on the discrete changes in the cell status (e.g., cell apoptosis) by introducing discontinuity into solution of corresponding equation (smoothed numerically). The carcinogen accumulates in cells as time goes on. The mutation flag in the CA model is switched on as soon as the carcinogen concentration passes the threshold level. Various types of carcinogens (e.g., arsenic absorbed from the drinking water or aromatic acids

– byproducts of cigarette smoking) have different DNA mutation thresholds [19]. The model could be adapted for each type of the major carcinogen by varying this parameter.

Following the chain of mutations the cell could obtain "invasive phenotype" (MMP-flag equal to one) and as result the MMP secretion is started. The probability of such event could be extracted based on the epidemiological data for BC [17]. This flag signals beginning of execution of the continuous model of MMP-TIMP interaction described by Eqs. (1)–(4).

The system (1)–(4) is solved using the initial conditions received from the CA model as discussed in section 3.6. The results of the MMP-TIMP interaction model execution are transferred to the CA algorithm in order to update the cell state vector (level of the ECM degradation by MMP given by $k_6 ur$ in Eq. (4) and subsequent direction of tumor progression). The model interaction mechanism is charted in Fig. 4.

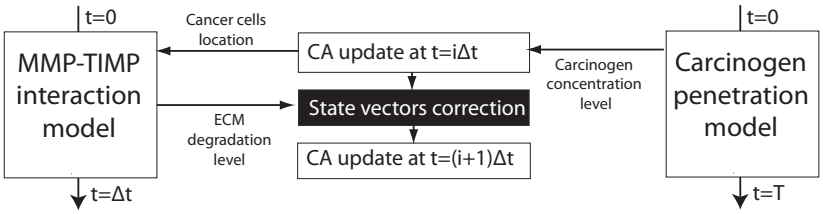

FIGURE 4. Hybrid model of invasive BC

Continuous both in space and in time penetration process goes through all simulation period (from $t = 0$ to $t = T$) as discussed in [18]. It depends on the randomly changing carcinogen concentration on the bladder wall and porosity properties of the different layers of urothelium. On the other hand, the simulation of MMP-TIMP interaction starts when the first cell obtains invasive phenotype only and it runs between two CA time steps (ΔT). The MMP-TIMP interaction model keeps accumulating values of MMP and TIMP concentrations (u and v correspondingly) from the previous time-steps for all computational domain. However, it obtains new tumor and tissue density maps (n and r correspondingly) as initial conditions on every new CA time-step. The state vector correction is done with accordance to the ECM degradation level submitted by the MMP-TIMP model.

5. **Numerical simulations.**

5.1. **Assumptions and simplifications.**

As any mathematical model of the complex biological process our combined model includes the number of assumptions and simplifications. Their goal is to make model easy for understanding and setup computer simulations without missing the most important biological features of tumor development and progression. The list bellow connects the mathematical model discussed above with biological background and could be reduced in future high-fidelity models.

- The tissue is well oxygenated. We consider that both tumor and regular cells receive sufficient oxygen through diffusion that illuminating cell apoptosis due to hypoxia.

- The angiogenesis hasn't started yet or its influence is still negligible during the simulated period of time. The previous assumption allows as to consider the effects of angiogenesis as minor. The experimental results [15] also confirm that effect of angiogenesis becomes visible on the later invasion stages.
- In fact, see also [25] for experimental results, the mutated cells are sending signals to the adjusted to tumor stromal cells (the stem cells which aren't level bound). These cells are secreting MMP. The effect is, in particular accounted for by using an assumption that only borderline tumor cells are secreting enzymes.
- The carcinogen penetration is stopped (or significantly slowed down) by the tissue membrane. Penetration of carcinogen to the muscle and fat layers could probably lead to mutations and development of the secondary tumors, however this process has no confirmation in the literature and is not modeled in this work.
- The natural turnover time of urothelial cells is approximately one year. It is much shorter than the lifespan of the muscle and fat cells, which is experimentally confirmed to be "infinite" or almost infinite compared to the urothelial cells [12]. On the other hand, the cells forming blood vessels are turning over in much faster pace (by few orders of magnitude) than the urothelial cells. Within our time-scale we assume that the ECM degradation following the MMP secretion is the only pathway for the apoptosis of the basal lamina, muscle and fat cells.
- Geometry of the cell is neglected (all cells are considered as identical squares.
- We refer to [18] for discussion related to the biological assumptions related to the penetration of the carcinogens through urothelium.

5.2. **Computations.** We simulate invasive BC on the one-cell-thick layer of the urothelium, which is, in fact, a two-dimensional lattice. We present three possible scenarios of tumor behavior. The major difference between the scenarios is the relation between the model parameters. All parameters have the same or similar order of magnitude as other mathematical models of invasive processes involving chemotaxis [8, 30]. We choose 8 years as the lifespan for all simulations. We consider this time to be sufficient for development of the invasive form of BC. It corresponds to the number of DNA mutations (4–5) necessary to develop a corresponding to the BC cancerous phenotype. The most important parameters defining the properties of invasion are the rate coefficients $k_1 ... k_6$. They correspond to the cancer cell proliferation rate (k_1), secretion and neutralization of MMP (k_2 and k_3 correspondingly), production of TIMP (k_4) and growth and degradation of invaded tissue (k_5 and k_6 correspondingly). In the computational tests presented in this work, we regulate k_2 and k_4 as their balance could give us insight into the speed and depth of the tumor progression. These coefficients are also indirectly targeted in both pre-clinical development and trials of cancer therapies as discussed in Section 6.

The most common scenario of invasive BC is when the tumor progression is limited by the muscle and fat and doesn't go beyond the layers surrounding the urothelium (stage T2 in Fig.2) [17]. This scenario is shown in Fig. 5. The plot shows progression of the major tumor suppressed (or significantly slowed down) by the TIMP. The tumor is surrounded by the thin envelope of the degraded cells and its expected development is in the horizontal rather than in the vertical direction. Such tumors are removed surgically and they usually don't require subsequent chemotherapy treatment.

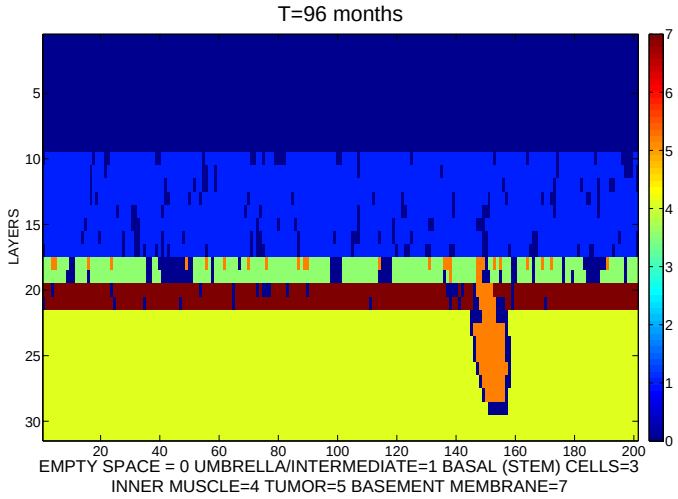

FIGURE 5. **Scenario 1**. Simulation parameters: $D_n = 10^{-5}$, $D_u = 5 \times 10^{-3}$, $D_v = 10^{-3}$, $\kappa = 2.5 \times 10^{-3}$, $k_1 = k_2 = k_3 = 10 = k_5 = 10$, $k_4 = 150$, $k_6 = 100$.

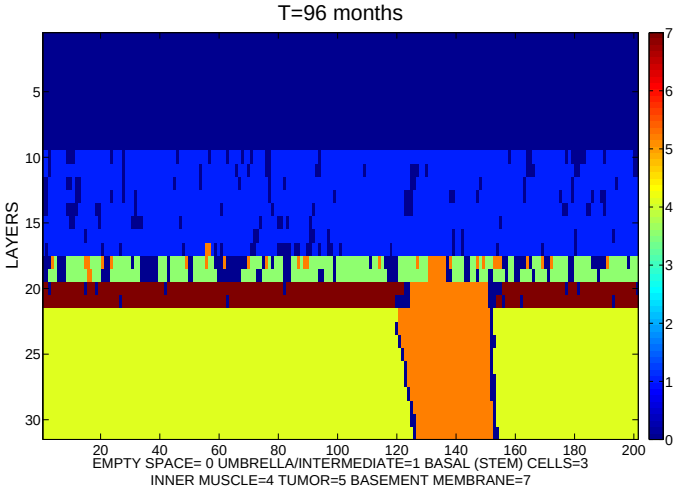

FIGURE 6. **Scenario 2**. Simulation parameters: $D_n = 10^{-5}$, $D_u = 5 \times 10^{-3}$, $D_v = 10^{-3}$, $\kappa = 2.5 \times 10^{-3}$, $k_1 = ... = k_5 = 10$, $k_6 = 100$.

The next scenario shows the spread of the tumor to the the tissues beyond the urothelium (stages T3 and T4 in Fig. 2). This simulation as it is seen from Fig. 6 shows the most dangerous type of the tumor, which passed through the surrounding urothelium tissues and continues its development. The treatment of BC on this stage almost always involves surgery followed by the chemotherapy and could require surgical removal of bladder. The angiogenesis starts playing an

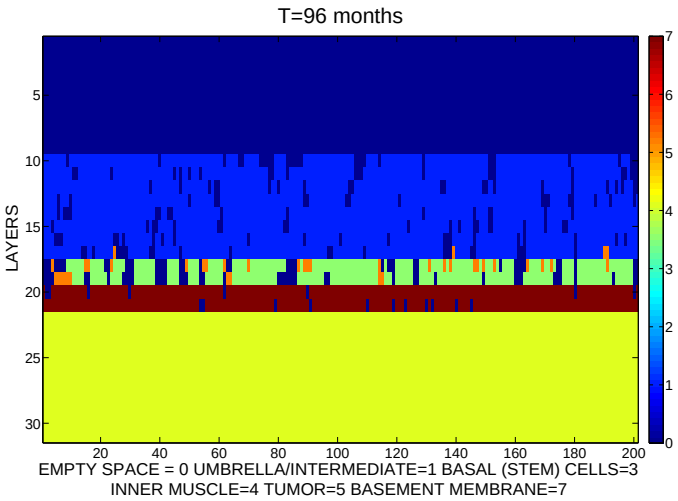

FIGURE 7. **Scenario 3**. Simulation parameters: $D_n = 10^{-5}$, $D_u = 5{\times}10^{-3}$, $D_v = 10^{-3}$, $\kappa = 2.5{\times}10^{-3}$, $k_1 = k_3 = k_4 = k_5 = 10$, $k_2 = 0.1$, $k_6 = 100$.

important role on this stage of tumor development and could be a major factor in direction of its progression as well as in determination of its speed.

The third scenario, which snapshot is presented in Fig. 7 deals with the situation when the invasion is stopped by the TIMP and small clones of the cancerous cells are confined to the lower levels of urothelium. This type of low grade tumors usually remains undiagnosed. However, the multiple clones of mutated cells visible on this plot could eventually start carcinoma in situ or superficial BC (stages Ta and T1 in Fig. 2) [18]. In addition, any traumatic event (e.g., bladder injury) could lead to the speed up in cell proliferation and as result to the development of invasive tumor as shown in Scenarios 1 and 2

Our results show that by changing the rate coefficients we could simulate various situations, which in turn could lead to different outcome and the as result to require different surgical involvement and/or anti-cancer therapy. The simulations presented above use k_2 and k_4 as the parameters involved into MMP and TIMP producing. Additional rate coefficients combinations would lead to the more complex scenarios and worth study in the framework of the therapy modeling. The ECM degradation coefficient leading to the apoptosis is set to be equal to 0.75 in all simulations (see [19] for the corresponding discussion). One interesting model observation, which corresponds to *in vivo* results, is an existence of the multiple cancerous cells spread through the urothelium, which lead to one (as in the Figs. 5 and 6) or two primary tumors only. In fact, most cancerous cells cannot develop into tumor, as they eventually die due to hypoxia and lack of the nutrients.

6. **Conclusions.** The goal of this work is to build a computational tool for modeling invasive BC. The quantitative simulations show agreement with the qualitative observations and could be employed for analysis of the BC growth in parallel with in vitro experiments. Tumor-bladder interaction is very complicated and its full mathematical description seems to be impossible. However, there is a well known

need from the medical community in computer simulation of major mechanisms behind BC progression and tissue response.

The hybrid discrete-continuous framework chosen in this work has shown itself as a very intuitive and convenient way to describe complex biological processes on both cellular and tissue levels. The model presented in this work is very adaptive, as both state vector and CA rules could be updated to describe various phenomena in cellular behavior. In particular, they could arise as a response of urothelial cells to the hypoxia and the angiogenesis (driven by corresponding continuous models) or as a reaction of tumor on the different therapy strategies

Discussed in this work MMP secretion has long been heralded as a promising target for cancer therapy on the basis of its massive up-regulation in malignant tissues and its unique ability to degrade all components of the ECM. Preclinical studies testing the efficacy of MMP suppression in tumor models were so compelling that synthetic metalloproteinase inhibitors (MPI) were rapidly developed and routed into human clinical trials. However no one of them was approved by the FDA as the results of clinical trials where considered unconvincing (see [9] for discussion). Despite this fact, this direction is still regarded very promising and our model could be used for the MMP suppression therapy simulation.

Another highlight of the continuous part of our model belongs to the TIMP production by the invaded tissue. Endogenous TIMP are multifunctional proteins that possess different MP-inhibitory activities and divergent other functions. Their attributes may be exploited in the search for novel therapies like increasing the local concentration of TIMP. So far technical difficulties prevented development of TIMP stimulators into useful drugs for cancer and other diseases. However, detailed analysis of the clinical trials [4] shows that following recent progress in clinical research their results should be re-considered and new set of clinical trials should be started. Our computational approach could become a part of the theoretical studies of this type of therapy.

Adding of angiogenesis component to the model, for instance using approach discussed in [23] would be an important step in modeling anti-angiogenic therapy – another promising direction in BC treatment.

Finally, we want to point out that the BC development and growth has its own features as discussed in this work, however, it also has common characteristics with the number of cancers developing in the transitional tissue (epithelium). This means that our hybrid model could be converted and exploited for modeling other types of cancer and eventually various cancer therapies.

REFERENCES

[1] A. E. Anderson, *A hybrid mathematical model of solid tumour invasion: The importance of cell adhesion*, Mathematical Medicine and Biology, **22** (2005), 163–186.

[2] F. Andreu, V. Caselles and J. Mazan, *Diffusion equations with finite speed of propagation*, in "Functional Analysis and Evolution Equations" (eds. H. Amann et al), Birkhauser Basel, (2008), 17–34.

[3] Atlas of Genetics and Cytogenetics in Oncology and Haematology, `http://AtlasGeneticsOncology.org`. Image available for use under CCA license.

[4] A. H. Baker, D. R. Edwards and G. Murphy, *Metalloproteinase inhibitors: Biological actions and therapeutic opportunities*, J. of Cell Science, **115** (2002), 3719–3727.

[5] C. E. Brinckerhoff and L. M.Matrisian, *Matrix metalloproteinases: A tail of frog that became a prince*, Nature Reviews, Molecular Cell Biology, **3** (2002) 207–214.

[6] H. M Byrne, M. A. J. Chaplain, G. J. Pettet and D. L. S. McElwain, *A mathematical model of trophoblast invasion*, J. of Theor. Medicine, **1** (1999), 275–286.

[7] C. Chang and Z. Werb, *The many faces of metalloproteases: cell growth, invasion, angiogenesis and metastasis*, Trends in Cell Biology, **11** (2001), 37–43.
[8] M. A. J. Chaplain and G. Lolas, *Mathematical modeling of cancer invasion of tissue: Dynamic heterogeneity*, Networks and Heterogeneous Media, **1** (2006), 399–439
[9] L. M. Coussens, B. Fingleton and L. M. Matrisian, *Matrix metalloproteinase inhibitors and cancer: Trials and tribulations*, Science, **295** (2002), 2387–2392.
[10] G. B. Ermentrout and L. Edelstein-Keshet, *Cellular automata approaches to biological modelling*, J. Theor. Biol., **160** (1993), 97–133.
[11] R. A. Gatenby and E. T. Gawlinski, *A reaction-diffusion model of cancer invasion*, Cancer Research, **56** (1996), 5745–5753.
[12] B. George, R. H. Datar and R. J. Cote, *Molecular biology of bladder cancer: cell cycle alterations*, in "Textbook of Bladder Cancer" (eds. S. P. Lerner, et al), Taylor & Francis, (2006), 107–122.
[13] G. Giannelli, J. Falk-Marzillier, O. Schiraldi, W. G. Stetler-Stevenson and V. Quaranta, *Induction of cell migration by matrix metalloprotease-2 cleavage of lamitiin-5*, Science, **277** (1997), 225–228.
[14] F. Graner and J. A. Glazier, *Simulation of biological cell sorting using a two-dimensional extended Potts model*, Phys. Rev. Lett., **69** (1992), 2013–2016.
[15] G. P. Hemstreet III and E. M, Messing, *Early detection for bladder cancer*, in "Textbook of Bladder Cancer" (eds. S. P. Lerner, et al), Taylor & Francis, (2006), 257–266.
[16] A. Jemal, F. Bray, M. M. Center, J. Ferlay, E. Ward and D. Forman, *Global cancer statistics*, CA: A Cancer J. for Clinicians, **61** (2011), 69–90.
[17] T. Kakizoe, *Development and progression of urothelial carcinoma*, Cancer Science, **97** (1982), 821–828.
[18] E. Kashdan and S. Bunimovich-Mendrazitsky, "Multi-Scale Model of Bladder Cancer Development," Discrete and Continuous Dynamical Systems, 2011, 803–812.
[19] M. Kirsch-Voldersa, M. Aardemab and A. Elhajoujic, *Concepts of threshold in mutagenesis and carcinogenesis*, Mutation Res., **464** (2000), 3–11.
[20] C. J. Malemud, *Matrix metalloproteinases (MMPs) in health and disease: an overview*, Frontiers in Bioscience, **11** (2006), 1696–1701.
[21] B. P. Marchant, J. Norbury and J. A. Sherratt, *Travelling wave solutions to a haptotaxis-dominated model of malignant invasion*, Nonlinearity, **14** (2001), 1653–1671.
[22] C. J. Marshall, L. M. Franks and A. W. Carbonell, *Markers of neoplastic transformation in epithelial cell lines derived from human carcinomas*, J. Natl. Cancer Inst., **58** (1977), 1743–1751.
[23] L. L. Munn, C. Kunert and J. A. Tyrrell, *Modeling tumor blood vessel dynamics*, in "Mathematical Methods and Models in Biomedicine" (eds. U. Ledzewicz, et al), Springer, (2012), 113–142.
[24] G. Murphy and J. Gavrilovic, *The mathematical modelling of Proteolysis and cell migration: Creating a path?*, Curr. Opin. Cell Biol., **11** (1999), 614–621.
[25] K. Nabeshima, W. S. Lane and C. Biswas, *Partial sequencing and characterisation of the tumour cell- derived collagenase stimulatory factor*, Arch. Biochem. Biophys., **285** (1991), 90–96.
[26] U. 0. Nseyo and D. L. Lamm, *Immunotherapy of bladder cancer*, Seminars in Surgical Oncology, **13** (1997), 342–349.
[27] J. E. Nutt, G. C. Durkan, J. vK. Mellon and J. Lunce, *Matrix metalloproteinases (MMPs) in bladder cancer: The induction of MMP9 by epidermal growth factor and its detection in urine*, BJU International, **91** (2003), 99–104.
[28] A. J. Perumpanani, J. A. Sherratt, J. Norbury and H. M. Byrne, *A two parameter family of travelling waves with a singular barrier arising from the modelling of extracellular matrix mediated cellular invasion*, Physica D, **126** (1999), 145–159.
[29] V. Quaranta, K. A. Rejniak, P. Gerlee and A. R. A. Anderson, *Invasion emerges from cancer cell adaptation to competitive microenvironments: Quantitative predictions from multiscale mathematical models*, Seminars in Cancer Biology, **18** (2008), 338–348.
[30] I. Ramis-Conde, M. A. J. Chaplain and A. R. A. Anderson, *Mathematical modelling of cancer cell invasion of tissue*, Mathematical and Computer Modelling, **47** (2008), 533–545.
[31] C. J. Sherr, *Cancer cell cycles*, Science, **274** (1996), 1672–1677.
[32] W. G. Stetler- Stevenson, S. Aznavoorian and L. A. Liotta, *Tumor cell interactions with the extracellular matrix during invasion and metastasis*, Ann. Rev. Cell Biol., **9** (1993), 541–573.

[33] J. Testa, *Loss of metastatic phenotype by a human epidermoid carcinoma cell line hep-3 is accompanied by increased expression of tissue inhibitor of matrix metalloproteinase-2*, Cancer Res., **52** (1992), 5597–5603.
[34] Transitional epithelium of the urinary bladder, http://en.wikipedia.org/wiki/Urothelium. Image available for use under CCA license.
[35] S. Turner and J. A. Sheratt, *Intercellular adhesion and cancer invasion: A discrete simulation using the extended potts model*, J. Theor. Biol., **216** (2002), 85–100.
[36] K. Vasala, P. Paakko and T. Turpeenniemi-Hujanen, *Matrix metalloproteinase-9 (MMP-9) immunoreactive protein in urinary bladder cancer: A marker of favorable prognosis*, Anticancer Research, **28** (2008), 1757–1762.
[37] J. L. Vasquez, "Porous Medium Equation. Mathematical Theory," Oxford University Press, Oxford, 2007.
[38] S. M. Wnek, M. K. Medeirosa, K. E. Eblinb and A. J. Gandolfi, *Persistence of DNA damage following exposure of human bladder cells to chronic monomethylarsonous acid*, Tox. and Appl. Pharm., **241** (2009), 202–209.

Received June 06, 2012; Accepted November 18, 2012.

E-mail address: ekashdan@post.tau.ac.il
E-mail address: svetlanabu@ariel.ac.il